4 Results

We will present only plots of long-term average results in this section. These will take the form of either: (a) concentrations averaged over the entire duration of a simulation, (b) or ratios of the time-and-depth-averaged concentration for a chosen characteristic in paired simulations. These long-term averages provide an easily-grasped summary of results, but mask substantial short-term variability (due to wind-driven changes in the circulation patterns). We briefly discuss a few examples of this variability.

4.1 Interpretation of the plots

In all the plots of the raw results (concentrations of organisms), colour is indicative of abundance: rust-red indicates high abundance, whilst deep blue indicates low abundance. For snapper and plankton, the reported concentrations (and concentration ratios) are averages over sea-surface to sea floor and the full duration of the simulation. For the biophysical model, the averaging is over the upper 20 m the water-column and the full duration of the simulation. For the snapper and logistic plankton models we adopt a linear colour-scale when representing concentrations. For the biophysical model, colour is indicative of $\log_{10}$(concentration).

We also use colour-plots to illustrate the relative difference between the results of two farm scenarios (e.g., scenario 0 vs scenario NF). In this case, the colour is indicative of the ratio of long-term depth-average concentrations for corresponding properties as simulated under the two scenarios. This ratio provides a measure of the magnitude relative change that the farm activities are predicted to induce. As an alternative, one might have choose to examine the absolute magnitude of change. We have chosen the former measure because we believe it has greater intuitive appeal, and because it has been proposed that farm activities be regulated in relation to the degree of relative change that they induce. Nonetheless, it is important to realise that, where the 'natural' (*ie* farm-free) abundance of an organism is low, even a very small farm-associated change in abundance will correspond to a large relative change. If the population is abundant elsewhere in the system, the large local relative change (but small absolute change) may prove to be irrelevant.

Once again, we adopt linear colour-scales for the snapper and logistic models and logarithmic scales for the biophysical model. The plot legend and associated colour-scale bar will define the ratio in greater detail, but in all the cases it is calculated as the quotient: 'concentration in the simulation with many farms' / 'concentration in the simulation with few farms' (e.g., scenario 0/scenario NF or scenario 1/scenario NF). Since each farm-scenario was started from identical initial conditions, the ratio is always equal to one at the start of the simulation. Thereafter, areas which have a colour towards the blue end of the colour-spectrum are predicted to have lower

concentrations in the 'many farms' simulation than they do in the 'few farms' one. Conversely, areas having a colour towards the rust-red end of the spectrum have concentrations that are little different, or in some cases, higher than those of the no farms scenario.

Results will be presented in the order: snapper model, logistic plankton model, biophysical model. For each of these three models, the seasonal simulations will be presented in the following order: September 1999, March 2000, spring prevailing ENE winds, summer prevailing ENE winds, spring prevailing WSW winds, summer prevailing WSW winds. Finally, within each wind-scenario, results will be presented in farm-scenario order (*viz,* scenario NF, scenario 0, scenario 1).

It is important to remember that in all three models, the plankton (and fish eggs/larvae) are represented by collections of particles. Particle transport is driven by a combination of super-grid-scale advective transport (dictated by the current fields simulated by the hydrodynamic model) and sub-grid scale eddies – simulated as a random increment (direction and speed) to the deterministic velocity. This random component implies that, even if two particles start from the same location, their trajectories will tend to diverge. Recall further that plankton concentration within any region is derived from the sum of the plankton mass associated with each particle within the region and the volume of water within the region. Clearly, if there are few particles in a region, the addition (or loss) of just one particle will induce a large relative change in abundance – even if the absolute change in abundance is small. Given the random component in particle trajectories, this implies that concentration estimates become progressively less robust as the number of particles involved falls. Thus, the depth averaged concentration estimates reported in the remainder of this document are generally less robust in shallow areas of the firth than they are in deep areas. Similarly, and more importantly, relative changes in concentration (whether over time, or at corresponding times in differing farm scenarios) become more liable to 'sampling error' effects in shallow regions. For these reasons, even seemingly large depletion (or enhancement) effects should be considered meaningful only if they extend to several adjacent grid-cells or if they persist over a prolonged period of time in one cell. For example, in the shallow, southern firth it is not uncommon to see a 'speckled pattern' of alternating areas of high and low relative abundance, or a band of persistently high relative abundance. Both are artefacts arising from sampling error and is not evidence of far-field impacts upon biomass in the southern firth. As a very rough rule of thumb, we suggest that ratios derived from the long-term average concentrations should be regarded as unreliable in areas where the water depth is less than approximately 3 m (equating to areas in which the hydrodynamic model has only one layer). If shorter time-averaging periods were to be used, this depth threshold would be larger. Recall, also that the local particle abundance will be influenced by the absolute plankton abundance as well as water depth. For this reason ratios will be unreliable in deeper water if the plankton abundance is low (witness the band of seemingly enriched snapper larvae at the extreme southern edge of the snapper larval distributions in Figure 2).

4.2 Snapper Model

For the no farms situation, the 'long term average' (i.e., averaged over the duration of each simulation) simulated abundances of 7-8 d post-spawn snapper larvae are illustrated in Figure 2a. Relative deviations from these patterns under scenarios 0 and 1 are presented as in Figure 2b-c. Similarly, the deviations under the assumption of neutral buoyancy are plotted in Figure 2d (ENE winds only). The average spatial distribution varies markedly not only between different wind fields (Sept. 1999, March 2000, ENE and WSW winds), but also when the same winds are blown in different seasons (ENE spring, ENE summer, WSW spring, WSW summer). This is despite the fact that the spatial distribution of newly spawned eggs remained constant across all simulations (Figure 2 e).

On average, the Wilson bay development is predicted to induce only mild depletion (usually <10%, and often barely detectable) among 7-8 d old larvae. Addition of the western firth AMA induces much more marked depletion – frequently circa 20% over much of the southern and central firth. We note that this depletion is usually most marked in areas where natural larval densities are low. Thus, the spatial extent of larval depletion gives a deceptively large impression of the proportion of firth-wide fraction of eggs/larvae that may succumb to mussel grazing (see next paragraph for more details). Furthermore, we caution that two features of the model are likely to lead to over-estimation of the mortality rates induced by mussels. We will delay a description of these features until the Discussion.

Simulations indicate that when averaged over the entire domain, the mortality induced by scenario 1 mussel consumption amounts to ~5% of the 'natural mortality' (assuming snapper eggs & larvae to be no less vulnerable to mussel predation than phytoplankton, Table 6). The model suggests that the existing farms (those of scenario 0) may be responsible for reducing the domain-wide number of snapper (sub-class 3, relative vulnerability=0.25) reaching age 7 d (post spawn) by approximately 2% (Table 7). The combination of the existing farms and the maximal western firth development (scenario 1) is suggested to reduce the numbers of snapper (sub-class 3) reaching age 7 d by approximately 3-6%. Comparison of these figures with the mortality ratios in Table 6 suggests that, if eggs/larvae are, instead, as vulnerable as phytoplankton, the numbers of larvae reaching age 8 d could be reduced by ~6% under scenario 0 and ~ 15% under scenario 1. Note, however this will be an overestimate if snapper eggs or larvae are less vulnerable to mussel predation than phytoplankton are.

The distribution of depletion in 7-8 d old neutrally buoyant larvae is very different from that of slowly ascending larvae (Figure 2d *cf* Figure 2c). Note that the substantial decline in larval abundance in the with-farms, rapidly ascending case relative to the no-farms, slowly ascending case is primarily due to the changed pattern of horizontal distribution consequent upon the changed ascent speeds. This is made more evident

if we compare 'like-with-like' (by comparing the numbers of larvae attaining 8 d post-spawn under the differing farming scenarios, but making the comparison only across simulations in which eggs and larvae were assumed to have the same ascent speeds). This reveals that the fraction of eggs surviving to age 8 d is not strongly influenced by the ascent speed (Table 8). This is probably because, the initial distribution of eggs is identical in both populations, so earlier in their lives, all populations suffer similar levels of farm-induced mortality.

Figure 2:

Simulated concentrations (individuals m^{-3}) of 7-8 d old larval snapper under scenario NF (a), relative differences between the concentrations for the scenario NF/scenario 0 (b), scenario 1/NF (c). (d) relative deviation between results for scenario1, neutrally buoyant eggs/larvae and scenario NF, weakly buoyant eggs/larvae; ENE winds only). The top-most row also shows the time-series averaged abundance of snapper eggs<1 d old under Sept 1999 conditions (Figure 2e).

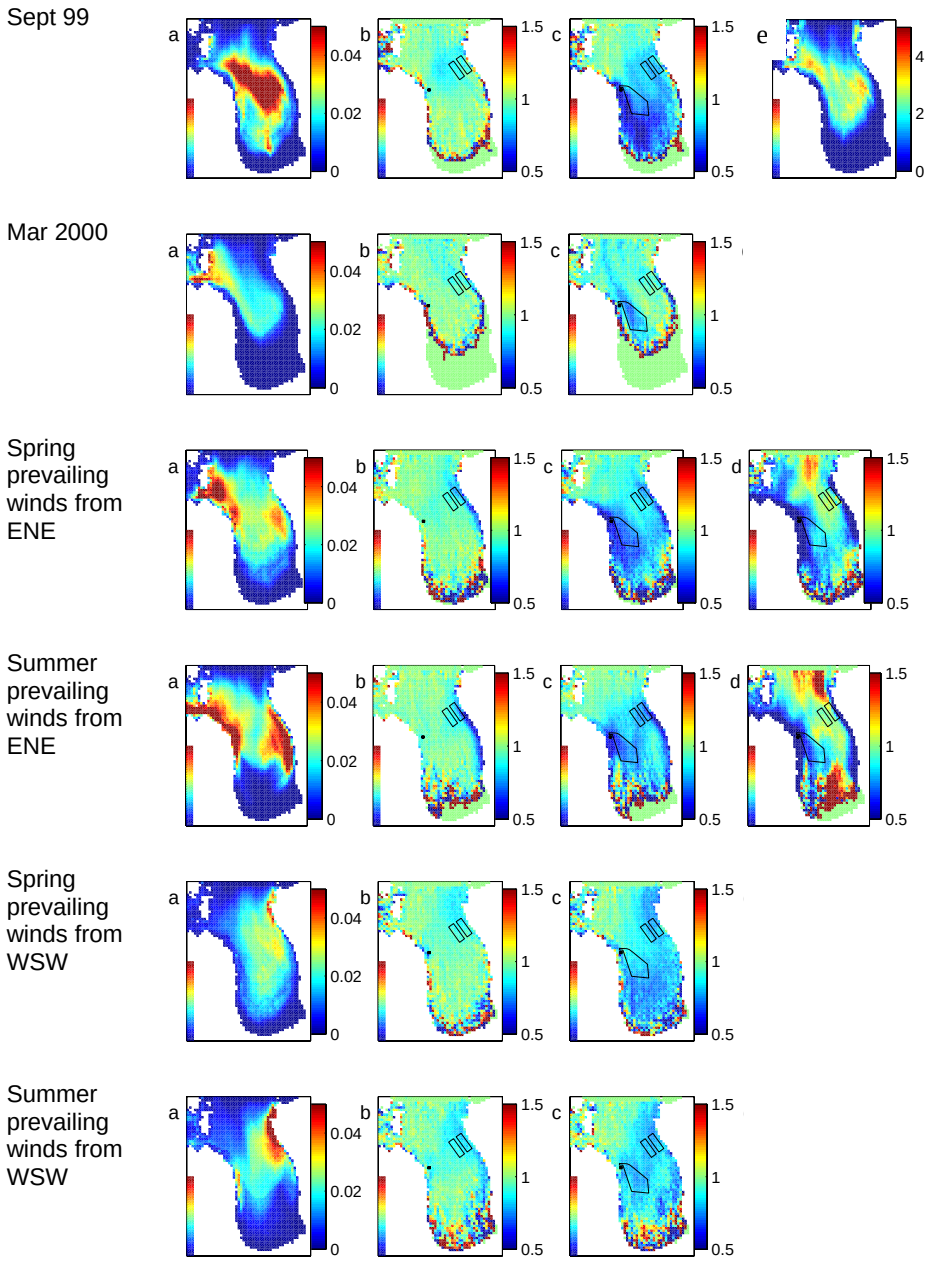

Table 6:

Ratios of domain-wide numbers eggs & larvae consumed by mussels to domain-wide total numbers of eggs and larvae dying due to background mortality (based upon totals accumulated over the entire duration of the simulation).

Season/wind	Scenario 0 Sub-class 1	Scenario 1 Sub-class1	Scenario 0 Sub-class 3	Scenario 1 Sub-class 3
September 1999	0.0175	0.0519	0.0046	0.0139
March 2000	0.0155	0.0464	0.0041	0.0124
Spring ENE	0.0162	0.0496	0.0043	0.0133
Summer ENE	0.0157	0.0496	0.0042	0.0135
Spring WSW	0.0240	0.0495	0.0063	0.0130
Summer WSW	0.0263	0.0518	0.0069	0.0137

Table 7:

Ratios of domain wide numbers of larvae attaining the assumed age of invulnerability (8 d) accumulated over the entire duration of the simulation. These ratios are for snapper sub-class 3 (relative vulnerability=0.25). Default model (snapper ascent speed=1 m d^{-1}).

Season/wind	scenario 0 / scenario NF	scenario 1 / scenario NF	scenario 1 / scenario 0
September 1999	0.982	0.943	0.960
March 2000	0.990	0.967	0.977
Spring ENE	0.987	0.948	0.961
Summer ENE	0.985	0.953	0.967
Spring WSW	0.983	0.950	0.966
Summer WSW	0.973	0.947	0.976

Table 8:

Ratios of domain wide numbers of larvae attaining the assumed age of invulnerability (8 d) accumulated over the entire duration of the simulation. These ratios are for snapper sub-class 3 (relative vulnerability=0.25) for two differing ascent speeds of eggs and larvae.

Season/wind	Ascent speed for non-motile eggs/larvae (m d^{-1})	scenario 0 / scenario NF	scenario 1 / scenario NF	scenario 1 / scenario 0
Spring ENE	0	0.987	0.954	0.967
Summer ENE	0	0.986	0.954	0.968
Spring ENE	5	0.978	0.942	0.963
Summer ENE	5	0.985	0.952	0.966